Published in final edited form as:
Exp Neurol. 2013 November ; 249: . doi:10.1016/j.expneurol.2013.08.003.

Phrenic motoneuron discharge patterns following chronic cervical spinal cord injury

Kun-Ze Lee[a,b], **Brendan J. Dougherty**[b,c], **Milapjit S. Sandhu**[b], **Michael A. Lane**[c], **Paul J. Reier**[c], and **David D. Fuller**[b,*]

[a]Department of Biological Sciences, College of Science, National Sun Yat-sen University, #70 Lien-Hai Rd., Kaohsiung 804, Taiwan

[b]Department of Physical Therapy, College of Public Health and Health Professions, McKnight Brain Institute, University of Florida, PO Box 100154, 100 S. Newell Dr, Gainesville, FL 32610

[c]Department of Neuroscience, College of Medicine, McKnight Brain Institute, University of Florida, PO Box 100244, 100 S. Newell Dr, Gainesville FL 32610

Abstract

Cervical spinal cord injury (SCI) dramatically disrupts synaptic inputs and triggers biochemical, as well as morphological, plasticity in relation to the phrenic motor neuron (PhMN) pool. Accordingly, our primary purpose was to determine if chronic SCI induces fundamental changes in the recruitment profile and discharge patterns of PhMNs. Individual PhMN action potentials were recorded from the phrenic nerve ipsilateral to lateral cervical (C2) hemisection injury (C2Hx) in anesthetized adult male rats at 2, 4 or 8 wks post-injury and in uninjured controls. PhMNs were phenotypically classified as early (Early-I) or late inspiratory (Late-I), or silent according to discharge patterns. Following C2Hx, the distribution of PhMNs was dominated by Late-I and silent cells. Late-I burst parameters (*e.g.*, spikes per breath, burst frequency and duration) were initially reduced but returned towards control values by 8 wks post-injury. In addition, a unique PhMN burst pattern emerged after C2Hx in which Early-I cells burst tonically during hypocapnic inspiratory apnea. We also quantified the impact of gradual reductions in end-tidal CO_2 partial pressure ($P_{ET}CO_2$) on bilateral phrenic nerve activity. Compared to control rats, as $P_{ET}CO_2$ declined, the C2Hx animals had greater inspiratory frequencies (breaths*min^{-1}) and more substantial decreases in ipsilateral phrenic burst amplitude. We conclude that the primary physiological impact of C2Hx on ipsilateral PhMN burst patterns is a persistent delay in burst onset, transient reductions in burst frequency, and the emergence of tonic burst patterns. The inspiratory frequency data suggest that plasticity in brainstem networks is likely to play an important role in phrenic motor output after cervical SCI.

Keywords

spinal cord injury; phrenic; motoneuron

*corresponding author: ddf@phhp.ufl.edu, Phone: +1-352-273-6634, Fax: +1-352-273-6109.

Introduction

The injured spinal cord is, in principle, a “new spinal cord” in which neural networks and control mechanisms affecting virtually every functional domain are altered (Dimitrijevic, 1998; Edgerton *et al.*, 2001). Accordingly, respiratory control mechanisms that have been firmly established in the spinal-intact condition are likely to be significantly altered after chronic spinal cord injury (SCI) (Sandhu *et al.*, 2009). A basic understanding of how SCI and spontaneous neuroplastic processes impact respiratory motor control is important for developing and optimizing spinal rehabilitation and repair approaches.

Much of our current understanding of respiratory motor plasticity following SCI derives from experiments which have utilized a lateral cervical (C2) hemisection model (C2Hx) (Goshgarian, 2003, 2009; Lane et al., 2008a; Sandhu et al., 2009; Zimmer et al., 2007). The C2Hx model has been used to carefully describe both the phrenic neurogram (*i.e.*, compound action potentials) and diaphragm electromyogram (EMG) recovery profiles after incomplete cervical SCI (reviewed in (Goshgarian, 2003, 2009; Sandhu *et al.*, 2009)). However, it is unknown whether the gradual and functionally incomplete recovery process after chronic cervical SCI (Dougherty *et al.*, 2012) coincides with fundamental changes in phrenic motoneuron (PhMN) recruitment profiles and discharge patterns (Lee and Fuller, 2011). In the spinal intact condition, respiratory-related PhMN bursting and recruitment is determined by both intrinsic motoneuron properties (*i.e.*, resistance, rheobase (Berger, 1979; Dick et al., 1987; Webber and Pleschka, 1976)) and descending (i.e., bulbospinal) and possibly propriospinal synaptic inputs (Monteau *et al.*, 1985). There is debate as to whether PhMN recruitment patterns during breathing are driven exclusively by membrane properties (*i.e.*, the “size principle” of motoneuron recruitment, (Henneman, 1957)), or if there is also some degree of selective synaptic input to cells recruited early *vs.* late in the inspiratory effort (reviewed in (Lee and Fuller, 2011)). In either case, since injuries to the cervical spinal cord are likely to alter both synaptic inputs (Goshgarian *et al.*, 1989) and intrinsic motoneuron properties (Mantilla and Sieck, 2009; Sperry and Goshgarian, 1993), fundamental changes in how the central nervous system regulates PhMNs are likely after cervical SCI.

Within the cervical spinal cord, neuroplastic changes occurring after C2Hx have been postulated to facilitate PhMN recruitment (Goshgarian, 2009; Tai et al., 1997a; Tai et al., 1997b) and lead to partial functional recovery. For example, increases in cervical spinal glutamatergic (Alilain and Goshgarian, 2008; Mantilla et al., 2012) and/or serotonergic receptor expression (Basura *et al.*, 2001; Fuller *et al.*, 2005; Mantilla *et al.*, 2012) could both serve to increase PhMN excitability. A similar functional impact could result from reductions in PhMN soma dimensions (Mantilla and Sieck, 2009), changes in dendrodentritic appositions, or increased number of synaptic active zones (Goshgarian, 2003; Goshgarian et al., 1989; Sperry and Goshgarian, 1993). The primary purpose of the present work was to to determine how whether PhMN discharge patterns and recruitment profiles are altered in a model of chronic, incomplete cervical SCI. Our overall hypothesis was that PhMNs would show a time-dependent increase in inspiratory burst frequency that paralleled the gradual recovery in phrenic motor output which follows C2Hx.

Materials and Methods

Animals

Male Sprague-Dawley rats were purchased from Harlan Inc. (Indianapolis, IN, USA). Rats were randomly assigned to the following groups: control, uninjured (N = 18, 388 ± 9 g, age 121 ± 4 days) or C2Hx injury. Rats with C2Hx were studied at 2 wks (N = 8, 327 ± 6 g, 108 ± 1 days), 4 wks (N = 8, 367 ± 7 g, 118 ± 2 days) or 8 wks (N = 7, 380 ± 15 g, 145 ± 3 days)

post-injury. All experimental procedures were approved by the Institutional Animal Care and Use Committee at the University of Florida.

Spinal cord injury

The C2Hx injury was induced at ~ 3 months of age (90 ± 1 day) as previously described (Dougherty et al., 2012; Lee et al., 2010; Sandhu et al., 2009), and the procedures are briefly summarized here. Rats were anesthetized by xylazine (10 mg/kg, s.c.) and ketamine (140 mg/kg, i.p., Fort Dodge Animal Health, IA, USA) and a dorsal incision was made from base of the skull to C3 spinal cord followed by C2 laminectomy and durotomy. A left C2Hx was then performed using a microscalpel followed by gentle aspiration. The dura, overlying muscles, and skin were closed and yohimbine (1.2 mg/kg, s.c., Lloyd, IA, USA) was given to reverse the anesthesia. Following the surgery, animals received an analgesic (buprenorphine, 0.03 mg/kg, s.c., Hospira, IL, USA) and sterile lactated Ringers solution (5 ml s.c.) injection. The post-surgical care protocol included daily injection of lactated Ringers solution (5 ml, s.c) and oral delivery of a nutritional supplement (Nutrical; 1 – 3 ml, Webster Veterinary, MA, USA) until adequate volitional drinking and eating resumed.

Neurophysiology

These methods were adapted from our prior reports (Lee *et al.*, 2009; Lee *et al.*, 2010) and are briefly reviewed here. Isoflurane anesthesia (3–4% in oxygen) was initially induced in a closed chamber, and then maintained via nose cone (2–3%). Rats were tracheotomized and mechanically ventilated (50–60% O_2, balance N_2; volume = 6–7 ml/kg; frequency = 60–70/minute throughout the experiment. Rectal temperature was monitored and maintained at 37.5 ± 1 °C by a servo-controlled heating pad (model TC-1000, CWE Inc., Ardmore, PA, USA). The femoral vein was catheterized (PE-50) for conversion to urethane anesthesia (1.6 g/kg, i.v., Sigma, St. Louis, MO, USA) and for injection of a paralytic drug (pancuronium bromide, 2.5 mg/kg, i.v., Hospira, Inc., Lake Forest, IL, USA). Another catheter was inserted into the femoral artery and connected to a pressure transducer (Statham P-10EZ pressure transducer, CP122 AC/DC strain gauge amplifier, Grass Instruments, West Warwick, RI, USA) for blood pressure measurement. The vagus nerves were sectioned to prevent ventilator entrainment. End-tidal CO_2 partial pressure ($P_{ET}CO_2$) was analyzed with a Capnogard CO_2 monitor placed on the expired line of the ventilator circuit (Novametrix Medical Systems, Wallingford, CT, USA) and regulated by adjusting ventilatory rate and/or inspired CO_2.

The phrenic nerves were isolated in the cervical region via a ventral approach and sectioned distally. Raw neural signals were recorded using monopolar silver hook electrodes and then amplified (1000x, Model 1700, A-M Systems, Carlsborg, WA, USA), band-pass filtered (0.3–10 kHz) and integrated (time constant 100 ms; model MA-1000; CWE Inc., Ardmore, PA, USA). Phrenic signals were digitized by a Power 1401 data acquisition interface and recorded on a PC using Spike 2 software (CED, Cambridge, England). After the first protocol (see below), the left phrenic nerve was stripped of connective tissue, desheathed, separated into small filaments and then replaced on the monopolar silver hook electrode as previously described (Lee *et al.*, 2009; Lee *et al.*, 2010). Electrical activity recorded from the phrenic filament was amplified (1000x, Model 1700, A-M Systems, Carlsborg, WA, USA) and band-pass filtered (0.3–10 kHz). Waveforms recorded were confirmed to represent action potentials from single PhMNs by using “spike sorting” function in Spike 2 software(Spike 2, CED) to ensure that both the waveform amplitude and shape had minimal, if any, variation throughout the duration of the recordings.

Experimental protocol

Two separate protocols were performed. The first protocol was designed to compare and contrast the CO_2 sensitivity of phrenic motor output on the ipsilateral and contralateral (to lesion) sides of the spinal cord. Thus, the electrical activity of both phrenic nerves was recorded with $P_{ET}CO_2$ initially set at 50 mmHg. After stable recordings were obtained, $P_{ET}CO_2$ was gradually reduced to 45, 40, 35 and 30 mmHg by increasing the ventilator rate and/or reducing inspired CO_2 concentration. Each $P_{ET}CO_2$ level was maintained for 2 minutes. The second protocol was designed to examine discharge pattern of PhMNs. Thus, the phrenic nerve ipsilateral to the lesion was carefully separated into small filaments as previously described (Lee *et al.*, 2009). This "fiber picking" approach was used to enable recording of action potentials from individual PhMNs (Kong and Berger, 1986; Lee et al., 2009; St John and Bartlett, 1981, 1985). Individual PhMNs were identified with $P_{ET}CO_2$ maintained at 50 mmHg. Thereafter, $P_{ET}CO_2$ was gradually reduced as in protocol 1. The $P_{ET}CO_2$ was then returned to 50 mmHg followed by three minutes of hypercapnia ($P_{ET}CO_2$ level = 70 – 80 mmHg). This hypercapnic challenge was used to examine whether previously silent PhMNs in the phrenic fiber recording could be recruited during higher respiratory drive.

Spinal cord histology

At the conclusion of the neurophysiological recording experiments, rats with C2Hx injury were systemically perfused with saline followed by 4% paraformaldehyde (Sigma, St. Louis, MO, USA). The cervical spinal cord was removed, cryoprotected and sectioned at 40 μm via a vibrotome. The spinal cord tissue sections were serially mounted on glass slides (Fisher Scientific, Pittsburgh, PA, USA) and stained with cresyl violet. Tissue sections were evaluated by light microscopy, and the extent of the complete lateral hemisections were histologically verified (Fuller *et al.*, 2009). Three rats with SCI were excluded from the data analysis when post-hoc histological analyses revealed an incomplete C2Hx (spared white matter in the ipsilateral C2 spinal cord).

Data analyses

Active PhMNs were classified as Early-I or Late-I type based on the discharge onset relative to the whole contralateral phrenic burst. PhMNs which start to discharge within initial 20 % of inspiratory duration (T_I) were defined as Early-I, and those that fired at > 20 % T_I were classified as Late-I (Lee and Fuller, 2011; Lee et al., 2009). PhMNs that were inactive during baseline and could only be recruited during hypercapnic challenge were defined as silent PhMNs. In addition, a novel PhMN discharge pattern was uncovered in C2Hx animals, characterized by tonic discharge throughout the respiratory cycle and higher discharge frequency during T_I. These PhMNs were defined as tonic discharge type. PhMN spikes were analyzed for discharge onset (*i.e.* the time difference between the first spike and the onset of the contralateral phrenic burst), the total number of spikes per respiratory cycle, the discharge duration (*i.e.* duration between first and final spike within each neural breath), and burst frequency (total spike number divided by discharge duration). For phrenic neurograms, T_I and expiratory duration (T_E) and phrenic inspiratory burst frequency were calculated as previously described (Lee *et al.*, 2009; Lee *et al.*, 2010).

Data were averaged over the final 30 seconds of each $P_{ET}CO_2$ level. Phrenic neurogram inspiratory burst amplitude was expressed relative to the peak response (% peak) detected in the initial protocol. All statistical tests were conducted to specifically examine our *a priori* hypotheses. A two-way repeated measures analysis of variance (ANOVA) followed by the Student-Newman-Keuls post hoc test was used to comparephrenic nerve activity. For assessment of burst amplitude within each time point, factor one was the side of the recording (i.e., ipsilateral or contralateral) and factor two was the level of $P_{ET}CO_2$.

Evaluation of burst amplitude across time points was done at baseline conditions (e.g., $P_{ET}CO_2$ = 50 mmHg) using a one-way ANOVA followed by the Student-Newman-Keuls post hoc test. The same test was used to compare PhMNs discharge (*i.e.*, onset time, spike number, discharge duration and frequency) across the experimental groups. All data are presented as the mean ± standard error. A P-value of < 0.05 was considered statistically significant for all analyses.

Results

Heart rate and blood pressure

Mean arterial blood pressure (MAP) was similar between control and C2Hx rats (Table 1). Furthermore, MAP declined in all groups when $P_{ET}CO_2$ was reduced (P < 0.01, Table 1). Heart rate (HR) was similar between experimental groups, but some modest differences were noted (Table 1). While uninjured control rats showed an increase in HR as MAP decreased (P < 0.01), HR did not change with declining MAP in rats studied at 2 wks post-injury (Table 1). However, at 4 wks post-injury, the HR responses to changes in $P_{ET}CO_2$ and/or MAP were similar to the control group.

PhMN discharge

A total of 75 PhMNs were recorded across the four experimental groups. Phenotypic classifications were made with $P_{ET}CO_2$ maintained at 50 mmHg to ensure inspiratory activity in the phrenic nerve ipsilateral to the injury. In uninjured animals, the majority (62%) of recorded PhMNs had an Early-I burst pattern (Fig. 1), and an additional 24% were classified as Late-I (Fig. 2). The remaining cells (14%) were considered ‘silent PhMNs’ as inspiratory bursting was absent when $P_{ET}CO_2$ was 50 mmHg (Fig. 3). Silent PhMNs that were activated by raised $P_{ET}CO_2$ in uninjured animals discharged with a Late-I pattern (Fig. 3).

A shift in the overall distribution of PhMN phenotype was evident following C2Hx. First, the proportion of recorded PhMNs classified as Late-I was substantially increased at 2 wks post-injury, and this increase was maintained at both 4 and 8 wks (Fig. 4). The delay between onset of inspiration and the initiation of Late-I bursting (i.e., discharge onset time, ms) was not altered by C2Hx (P = 0.592, Fig. 5A), but some differences in firing patterns were prominent following the injury. Specifically, the total number of spikes per neural breath was reduced at 2 and 4 wks post-injury (Fig. 5B), and duration of discharge was attenuated at 4 wks post-injury (Fig. 5C). Late-I spike frequency (Hz) within each neural breath was reduced in all C2Hx groups, but most prominently at 4 wks post-injury (P<0.01; Fig. 5D). In all of the experimental groups, Late-I PhMNs showed an expected reduction in burst frequency when $P_{ET}CO_2$ was reduced (Table 2).

Cells bursting with an Early-I phenotype comprised less than 15% of the total recorded PhMNs at 2–4 wks post-injury, with only a single example being obtained in the 2 wk group. The overall proportion of Early-I PhMNs increased slightly to 28% at 8 wks post injury, but this number remained considerably less than control. The burst onset tended to be delayed in Early-I cells after C2Hx (*i.e.*, onset later in the inspiratory effort), but was not significantly different from uninjured animals (P = 0.074, Fig. 6A). However, the number of Early-I action potential spikes per breath was significantly lower at both 4 wks (4.6 ± 0.4) and 8 wks (6.9 ± 0.7) post-C2Hx when compared to control values (11.8 ± 0.8) (P < 0.01, Fig. 6B). Similarly, Early-I PhMN discharge frequency at 4 wks post-C2Hx animals was lower than control animals (P < 0.05, Fig. 6D).

Following C2Hx, a highly unique response to reductions in $P_{ET}CO_2$ was observed in Early-I PhMNs, and this response did not fit with the previously established PhMN burst

classification schemes (Kong and Berger, 1986; Lee et al., 2009; St John and Bartlett, 1981, 1985). Specifically, in 50% of recorded Early-I PhMNs, rhythmic inspiratory bursting gradually became tonic when $P_{ET}CO_2$ was progressively reduced (Fig. 1B). Moreover, the tonic bursting pattern persisted even when inspiratory apnea was confirmed by complete cessation of inspiratory bursting in the phrenic nerve contralateral to the injury. Thus, these PhMNs continued to fire action potentials despite the apparent absence of inspiratory "drive". This response was unique to Early-I cells since all Late-I PhMNs in C2Hx animals completely ceased bursting during hypocapnia-induced apnea (Fig. 2B). Because the appearance of tonic activity made it impossible to discern inspiratory-related *vs.* tonic firing patterns, the impact of $P_{ET}CO_2$ on burst parameters (e.g., frequency, onset) in Early-I PhMNs was not quantified.

Another prominent impact of C2Hx on PhMNs was that a much greater proportion of cells within the ipsilateral pool were silent. Thus, the number of recorded PhMNs which did not show inspiratory bursting when $P_{ET}CO_2$ was 50 mmHg increased considerably in all C2Hx groups (Fig. 4). Similar to control animals, silent PhMNs in C2Hx rats burst with a Late-I pattern when activated with a hypercapnic stimulus (Figs. 3–4), however, aspects of their discharge patterns were altered. Specifically, the number of spikes per breath and the overall discharge duration were both reduced in all C2Hx groups ($P < 0.05$, Figs. 7B–C). Once activated, the burst frequency of silent cells in C2Hx rats was similar to control values ($P = 0.46$, Fig. 7D).

Tonic PhMN bursting was also occasionally observed during periods of normocapnic inspiratory activity (*e.g.*, Fig. 8). The discharge pattern of these cells showed a clear inspiratory modulation, but tonic bursting occurred throughout the respiratory cycle. This pattern occurred in 7% of recorded cells following C2Hx, but was never observed in control rats (Fig. 4), and has not been previously reported in this experimental preparation (Kong and Berger, 1986; Lee et al., 2009; St John and Bartlett, 1981, 1985).

Phrenic nerve burst amplitude

Similar to PhMN assessments, initial evaluations of whole nerve activity (i.e., compound action potentials) were made with $P_{ET}CO_2$ maintained at 50 mmHg. As expected, phrenic nerve activity in uninjured animals was qualitatively and quantitatively indistinguishable between the left (*i.e.*, homologous to ipsilateral) and right (*i.e.*, homologous to contralateral) sides of the spinal cord (Fig. 9A). Inspiratory phrenic activity ipsilateral to the lesion could be detected in the majority of injured animals (88 % of rats at both 2 and 4 wks post-C2Hx; 100 % of rats at 8 wks; see Figs. 9B and 9C). The peak "raw" amplitude of the ipsilateral phrenic inspiratory burst (*i.e.*, arbitrary units, a.u.) was significantly lower in C2Hx rats when compared to the homologous nerve in the control group ($P < 0.01$, Fig. 10A). Ipsilateral phrenic nerve activity was also reduced when bursting was expressed relative to contralateral phrenic burst amplitude. Specifically, at 2 wks (7 ± 2%), 4 wks (7 ± 3%) and 8 wks post-C2Hx (20 ± 6%) bursting was consistently less than control values (115 ± 28%, $P < 0.01$, Fig. 10B). The onset of the ipsilateral phrenic burst was delayed relative to the contralateral phrenic burst (Fig. 11) as previously reported (Fuller *et al.*, 2008; Lee *et al.*, 2010). However, a time-dependent change in burst onset was indicated at 8 wks post-C2Hx by ipsilateral activity occurring earlier in the inspiratory effort ($P < 0.05$ *vs.* 2 wk group; Fig. 11). Nevertheless, that burst onset remained considerably delayed relative to control values ($P < 0.01$, Fig. 11). Contralateral phrenic bursting was similar across all groups during the baseline condition ($P = 0.77$, Fig. 10C).

We next quantified the efferent phrenic nerve response to gradual manipulations in $P_{ET}CO_2$ over 30–50 mmHg, a range that could be expected to encompass values occurring during eupneic breathing (Olson *et al.*, 2001). In the spinal intact control group, left and right

phrenic output showed quantitatively and qualitatively indistinguishable responses to $P_{ET}CO_2$ change, as expected (Figs. 9A and 12A). Following C2Hx, however, the ipsilateral (left) phrenic inspiratory burst was consistently blunted compared to the contralateral (right) burst across the range of 30–50 mmHg $P_{ET}CO_2$ (Fig. 12).

Tonic activity was prominent in the ipsilateral phrenic nerve recording at all post injury time points (Fig. 9). This observation is consistent with the PhMN data (*e.g.*, Figs. 1 and 8), and probably indicates an adaptation to SCI similar to the "spasticity" described in other motor pools (see discussion and reference(Li *et al.*, 2004)). Tonic phrenic nerve activity was most clearly evident when $P_{ET}CO_2$ was reduced in C2Hx rats. Under these conditions, phrenic tonic burst activity is seen to persist across the entire respiratory cycle (*e.g.*, Fig. 9Ciii–Cv). This result is consistent with the PhMN spike activity as shown in Fig. 1.

Phrenic nerve burst frequency

Phrenic inspiratory frequency (bursts*min^{-1}) was similar across all groups when assessed at 50 mmHg $P_{ET}CO_2$, and all groups showed a gradual reduction in frequency as $P_{ET}CO_2$ decreased ($P < 0.01$, Table 3). However, differences in inspiratory burst frequency between control and C2Hx rats became apparent at lower values of $P_{ET}CO_2$. Specifically, frequency in both the 2 and 4 wk C2Hx groups was greater than corresponding control values when $P_{ET}CO_2$ level was maintained at 30 and 35 mmHg ($P < 0.05$, Table 3). In addition, the CO_2 apneic threshold appeared to be reset to a lower level following C2Hx. Thus, inspiratory apnea (*i.e.*, cessation of rhythmic phrenic bursting) occurred in the majority (82%) of control rats when $P_{ET}CO_2$ was lowered to 30 mmHg. However, apnea was harder to induce after C2Hx with a greater proportion of rats showing robust inspiratory activity when $P_{ET}CO_2$ was 30 mmHg. Overall, inspiratory phrenic activity was present in 63% and 50% of C2Hx rats at 2 and 4 wk post-injury, respectively, when $P_{ET}CO_2$ was 30 mmHg. This value was 71% at 8 wks post-C2Hx.

Discussion

The present results represent the first detailed analyses of PhMN firing patterns following chronic high cervical SCI. Using a C2Hx model, we observed that the distribution of PhMN bursting shifted from cells that predominantly initiated bursting early in the inspiratory effort (i.e., Early-I) to cells with a Late-I phenotype. Reductions in PhMN discharge duration and burst frequency were also prominent after C2Hx. In addition, a unique PhMN discharge pattern emerged after C2Hx in which tonic PhMN bursting was present not only during the respiratory cycle, but also periods of inspiratory apnea. These collective findings provide novel insights regarding phrenic motor control following chronic cervical SCI.

Impact of C2Hx on PhMN discharge patterns

Respiratory-related PhMN burst patterns have been extensively studied in a variety of species in the spinal-intact condition (see reference (Lee and Fuller, 2011) for a detailed review). Collectively, the literature indicates that inspiratory PhMN discharge patterns are not homogenous, but rather bursting can be separated into two groups based on the recruitment profile during inspiration. Thus, as in the current study (e.g., Figs. 1–2), PhMN can be phenotypically classified as Early-I or Late-I (Kong and Berger, 1986; Lee et al., 2009; St John and Bartlett, 1979). In addition, cells which are inactive during typical "eupneic" baseline conditions - a population which makes up the majority of PhMNs (Mantilla and Sieck, 2011) - are classified as silent (Lee and Fuller, 2011).

Prior to the current work only one investigation of PhMN burst patterns following cervical SCI had been published (El-Bohy and Goshgarian, 1999). This earlier report described

ipsilateral PhMN bursting in rats a few hours after a C2Hx lesion. The results indicated that during active induction of the crossed-phrenic phenomenon (e.g., during an asphyxic stimulus), the discharge frequency of both Early-I and Late-I PhMNs in the ipsilateral phrenic nerve was increased as compared to pre-injury recordings. In addition, previously silent PhMNs were recruited during intense respiratory stimulation, and these cells were primarily of the Late-I phenotype. A large body of literature documents progressive (e.g. weeks-months) neuroplastic changes in the cervical spinal cord (Alilain and Goshgarian, 2008; Goshgarian, 2003, 2009; Mantilla et al., 2012; Mantilla and Sieck, 2003; Rowley et al., 2005; Sieck and Mantilla, 2009) along with increases in ipsilateral phrenic motor output following chronic C2Hx (Goshgarian, 2003, 2009), and this makes it difficult to directly compare results of that prior study with the current data. Nevertheless, one striking similarity between the two studies is the predominance of Late-I PhMNs during inspiration. Accordingly, the Late-I PhMN phenotype may not be the result of ongoing neuroplasticity following C2Hx, but rather may be an immediate and sustained consequence of the loss of ipsilateral descending synaptic inputs to the phrenic motor pool (see below: *Mechanisms influencing PhMN activity*). In contrast, the prior study did not report tonic PhMN activity during the acute post-injury phase, and accordingly we suggest that the unique tonic PhMN discharge noted in this study reflects mechanisms associated with chronic SCI (see below: *Tonic PhMN bursting*).

Mechanisms influencing PhMN activity following chronic C2Hx injury

The mechanisms underlying phrenic motor recovery following incomplete cervical SCI can be broadly considered either as “spinal” or “supraspinal” (Golder and Mitchell, 2005; Golder et al., 2001; Zimmer and Goshgarian, 2007). It must be emphasized, however, that spinal and supraspinal plasticity following SCI are not mutually exclusive. Indeed, the literature has documented neuroplastic changes in both the cervical spinal cord (Alilain and Goshgarian, 2008; Fuller et al., 2003; Mantilla et al., 2012) and medulla (Golder et al., 2001; Zimmer and Goshgarian, 2007) after C2Hx, and it seems most likely that the time-dependent increases in phrenic bursting after injury reflect progressive changes in neuronal populations at both locations.

Within the spinal cord, changes in the intrinsic excitability of PhMNs could contribute to the observed changes in bursting patterns after C2Hx. For example, the majority of active PhMNs were recruited late in the inspiratory effort following C2Hx, and PhMN discharge frequency was reduced after C2Hx. Both of these observations could theoretically reflect a persistent reduction in the excitability of PhMNs. In other words, there could be a decrease in PhMN membrane resistance (increased rheobase current), and in accordance with Henneman’s size principle (Henneman *et al.*, 1965), these cells would require more excitatory synaptic input to reach threshold. While definitive testing of this possibility will require intracellular recordings (e.g., (Enriquez Denton *et al.*, 2012)), we hypothesize that decreased PhMN excitability does not explain the observed bursting patterns. Mantilla and colleagues suggested in a preliminary report that PhMN soma size decreases after C2Hx (Mantilla and Sieck, 2009), and molecular changes in and around PhMNs after C2Hx are also consistent with increased excitability (Goshgarian, 2009; Sperry and Goshgarian, 1993; Tai et al., 1997a; Tai et al., 1997b). In our opinion, the more likely scenario is that the decreased burst frequency and Late-I phenotype occur due to the dramatic reduction in bulbospinal synaptic inputs to ipsilateral PhMNs after C2Hx. Reduced excitatory synaptic input should make it more difficult for PhMNs to reach the threshold for action potentials during inspiration, thus delaying burst onset and diminishing burst frequency. This suggestion is supported by the observation that during the acute post-injury phase (i.e., 2 days post-C2Hx; before extensive neuroplasticity and/or anatomical remodeling), PhMNs have already adopted a primarily Late-I phenotype (El-Bohy and Goshgarian, 1999).

Progressive increases in PhMN excitability over weeks-months post-C2Hx, as suggested by prior work (Goshgarian, 2009; Tai et al., 1997a; Tai et al., 1997b) may offset the reduction in excitatory bulbospinal inputs to these cells, but without ever fully correcting the C2Hx-induced reductions in phrenic output.

Another consideration is that propriospinal interneurons contribute to the formation of *de novo* intraspinal circuits after SCI (Bareyre et al., 2004; Lane et al., 2009; Lane et al., 2008b). In the spinal-intact condition, it is generally accepted that monosynaptic innervation of PhMNs by respiratory bulbospinal axons provides the primary inspiratory-related drive (Ellenberger and Feldman, 1988; Ellenberger et al., 1990). For example, cross-correlation analysis has thus far failed to detect any evidence for inspiratory drive being relayed from cervical interneurons to PhMNs (Duffin and Iscoe, 1996), and inspiratory bursting patterns in cervical interneurons (Bellingham and Lipski, 1990) have generally been attributed to afferent and “integrative” pathways (Bellingham, 1999). However, there is clear evidence for anatomical connectivity between cervical interneurons and PhMNs normally (Lane, 2011), and after chronic C2Hx (Lane, 2011; Lane et al., 2008b; 1993). There is now growing evidence supporting the hypothesis that propriospinal cervical interneurons are part of the neuronal substrate for phrenic recovery after cervical SCI (Alilain et al., 2008; Lane et al., 2008a; Lane et al., 2009; Lane et al., 2012; Lane et al., 2008b; Sandhu et al., 2009). This hypothesis is based on the results of transynaptic labeling experiments (Lane, 2011; Lane et al., 2008b), neurophysiological data (Sandhu *et al.*, 2009), and evidence that propriospinal interneurons make a prominent contribution to motor function following SCI in other motor systems (Bareyre et al., 2004; Courtine et al., 2009; Courtine et al., 2008; Flynn et al., 2011; Harkema, 2008). Accordingly, it is possible that the alterations in PhMN burst patterns noted in the present study, including the delayed burst onset, may reflect the emergence of polysynaptic pathways to PhMNs following chronic SCI.

Active inhibition of PhMNs is another mechanism which could alter burst parameters following C2Hx. Indeed, several experiments have indicated that phrenic motor output after C2Hx is subject to inhibition by segmental afferent inputs (Goshgarian, 1981; Vinit *et al.*, 2007). For example, Goshgarian demonstrated that cutting the cervical dorsal roots triggered an abrupt increase in ipsilateral diaphragm activity in rats with C2Hx (Goshgarian, 1981). Accordingly, afferent neurons, possibly phrenic afferents (Vinit *et al.*, 2007), may constrain phrenic motor output following SCI. However, in the present study all rats received a bilateral phrenicotomy prior to neurophysiological measurement of phrenic activity, and accordingly ongoing activation of phrenic afferent neurons could not explain the observed PhMN burst patterns.

Supraspinal plasticity also occurs following C2Hx (Golder and Mitchell, 2005; Golder et al., 2001; Zimmer and Goshgarian, 2007), and is also likely to contribute to alterations in phrenic motor control. For example, Zimmer and Goshgarian demonstrated significant changes in glutamate, adenosine and neurokinin-1 receptors in the medulla of neonatal rats following C2Hx (Zimmer and Goshgarian, 2007). In adult rats, Golder and colleagues showed that hypoglossal inspiratory activity is changed after C2Hx, thereby proving that brainstem respiratory motor output can be changed following cervical SCI (Golder *et al.*, 2001). The best evidence for altered brainstem output in the present study comes from the observed changes in inspiratory phrenic nerve burst frequency (breaths*min^{-1}) after C2Hx. Since the neurophysiological recordings were made under conditions of vagotomy, phrenicotomy, and pharmacologically induced neuromuscular paralysis it is unlikely that differences in sensory afferent input between experimental groups underlies the observed differences in burst frequency. If supraspinal plasticity contributes to altered phrenic output, an important question is whether this plasticity affects only the overall respiratory rhythm, or if the observed patterns of PhMN bursting (e.g., delayed onset, altered burst frequency)

are being driven by changes in the brainstem. Alterations in intrinsic motoneuron properties following C2Hx represent the most likely candidate mechanism, but changes in the brainstem inputs, or changes in spinal synaptic connectivity cannot be ruled out.

Tonic PhMN activity after C2Hx

The most unique aspect of PhMN activity after C2Hx was the appearance of tonic burst patterns. Tonic bursting occurred in some PhMNs throughout the respiratory cycle, and in other cells it was observed during periods of inspiratory apnea. Tonic PhMN bursting could reflect loss of inhibitory synaptic inputs and/or the appearance of novel tonic excitatory inputs, or changes in intrinsic membrane properties. In the spinal intact condition, there is little evidence to support the prevalence of PhMN plateau potentials and persistent inward currents (PICs) that might lead to tonic bursting. For example, Enriquez-Denton and colleagues (Enriquez Denton *et al.*, 2012) recently recorded intracellularly from PhMNs in decerebrate cats, and plateau potentials were never observed when bulbospinal pathways were intact. However, an example of a PIC was found in a PhMN following a sagittal section of the caudal medulla which severed descending bulbospinal axons. In addition, plateau potentials were readily observed in expiratory thoracic motoneurons, even when bulbospinal pathways were intact. Interestingly, PICs in motoneurons are believed to be generated in large part due to the CaV1.3 calcium channel (Sukiasyan et al., 2009; Zhang et al., 2008), and Enriquez-Denton et al. observed that PhMNs were robustly immunopositive for these channels. The authors concluded that descending (i.e., bulbospinal) modulation of PICs may act to limit their presence in PhMNs. Accordingly, it is tempting to suggest that PICs (and associated tonic PhMN burst activity) could emerge after cervical SCI when many descending inputs are interrupted. A remarkable recent study by Murray et al. (Murray *et al.*, 2010) also sheds light on the associated mechanisms. Specifically, they reported that constitutive activation (*i.e.* activated without ligand binding (Costa and Herz, 1989; Murray et al.)) of serotonin (5-HT) type 2C receptors on spinal motoneurons emerged following chronic SCI (Murray *et al.*, 2010). The constitutive activation was associated with PICs and tonic bursting. The 5-HT2C receptor is expressed on and around PhMNs after cervical SCI (Basura *et al.*, 2001), and accordingly a similar mechanism could be evoked in the phrenic motor pool.

There are several additional plausible mechanisms which could contribute to the tonic PhMN bursting occurring after C2Hx. First, descending inhibitory inputs to PhMNs arise from the Bötzinger complex in the ventrolateral medulla (Stornetta et al., 2003; Tian et al., 1998). Interruption of these inputs following C2Hx could release PhMNs from inhibition and raise the probability of tonic bursting. However, this is unlikely since tonic bursting was not observed acutely after C2Hx (El-Bohy and Goshgarian, 1999). Another plausible mechanism is that the emergence of *de novo* intraspinal circuits (see above), could result in changes in PhMN excitability and contribute to tonic bursting. Tonic discharge patterns of cervical spinal interneurons have been described (Hayashi *et al.*, 2003; Lane *et al.*, 2009), although not after SCI. Regardless of the underlying cellular mechanisms, our data reveal that tonic burst patterns occur in a subset of PhMNs after chronic SCI, and rhythmic bulbospinal respiratory synaptic inputs can “override” such tonic bursting (e.g., Figs. 1 and 8). A final consideration is the use of urethane anesthesia in the current experiments. Anesthesia has been shown to prevent PICs in motoneurons (Enriquez Denton *et al.*, 2012), and accordingly, we may have in fact underestimated the prevalence of tonic PhMN bursting after SCI. Future studies can address this concern by utilizing a decerebrate preparation.

Conclusion

A unilateral cervical SCI which removes descending synaptic inputs to the ipsilateral phrenic motor pool (i.e., C2Hx) results in alterations in the recruitment patterns and burst

profiles of PhMNs. The delay in PhMN burst onset and reductions in burst frequency are likely to reflect the persistent reduction in bulbospinal excitatory synaptic inputs to the phrenic pool, although spinal neuroplasticity, including formation of *de novo* intraspinal circuits, may play a role. We hypothesize that the emergence of tonic burst patterns reflects changes in the intrinsic properties of PhMNs after chronic C2Hx. Lastly, plasticity in brainstem respiratory networks, as suggested by alterations in the overall respiratory frequency, is likely to play an important role in determining the overall respiratory rhythm after chronic cervical SCI.

Acknowledgments

Support for this work was provided by grants from the National Institutes of Health (NIH): 1R01NS080180-01A1 (DDF). KZL was supported by the Paralyzed Veterans of America Research Foundation (#2691), National Science Council (NSC) NSC100-2320-B-110-003-MY2, National Health Research Institutes (NHRI-EX102-10223NC) and NSYSU-KMU Joint research Project (2013-I006).

Abbreviations list

C2Hx	C2 spinal cord hemisection
Early-I	early-inspiratory
Late-I	late-inspiratory
PICs	persistent inward currents
$P_{ET}CO_2$	end-tidal CO_2 partial pressure
PhMNs	phrenic motoneurons
SCI	spinal cord injury
T_I	inspiratory duration
T_E	expiratory duration

References

Alilain WJ, Goshgarian HG. Glutamate receptor plasticity and activity-regulated cytoskeletal associated protein regulation in the phrenic motor nucleus may mediate spontaneous recovery of the hemidiaphragm following chronic cervical spinal cord injury. Exp Neurol. 2008; 212:348–357. [PubMed: 18534577]

Alilain WJ, Li X, Horn KP, Dhingra R, Dick TE, Herlitze S, Silver J. Light-induced rescue of breathing after spinal cord injury. J Neurosci. 2008; 28:11862–11870. [PubMed: 19005051]

Bareyre FM, Kerschensteiner M, Raineteau O, Mettenleiter TC, Weinmann O, Schwab ME. The injured spinal cord spontaneously forms a new intraspinal circuit in adult rats. Nat Neurosci. 2004; 7:269–277. [PubMed: 14966523]

Basura GJ, Zhou SY, Walker PD, Goshgarian HG. Distribution of serotonin 2A and 2C receptor mRNA expression in the cervical ventral horn and phrenic motoneurons following spinal cord hemisection. Exp Neurol. 2001; 169:255–263. [PubMed: 11358440]

Bellingham MC. Synaptic inhibition of cat phrenic motoneurons by internal intercostal nerve stimulation. J Neurophysiol. 1999; 82:1224–1232. [PubMed: 10482742]

Bellingham MC, Lipski J. Respiratory interneurons in the C5 segment of the spinal cord of the cat. Brain Res. 1990; 533:141–146. [PubMed: 2085725]

Berger AJ. Phrenic motoneurons in the cat: subpopulations and nature of respiratory drive potentials. J Neurophysiol. 1979; 42:76–90. [PubMed: 430115]

Costa T, Herz A. Antagonists with negative intrinsic activity at delta opioid receptors coupled to GTP-binding proteins. Proc Natl Acad Sci U S A. 1989; 86:7321–7325. [PubMed: 2552439]

Courtine G, Gerasimenko Y, van den Brand R, Yew A, Musienko P, Zhong H, Song B, Ao Y, Ichiyama RM, Lavrov I, Roy RR, Sofroniew MV, Edgerton VR. Transformation of nonfunctional spinal circuits into functional states after the loss of brain input. Nat Neurosci. 2009; 12:1333–1342. [PubMed: 19767747]

Courtine G, Song B, Roy RR, Zhong H, Herrmann JE, Ao Y, Qi J, Edgerton VR, Sofroniew MV. Recovery of supraspinal control of stepping via indirect propriospinal relay connections after spinal cord injury. Nat Med. 2008; 14:69–74. [PubMed: 18157143]

Dick TE, Kong FJ, Berger AJ. Correlation of recruitment order with axonal conduction velocity for supraspinally driven diaphragmatic motor units. J Neurophysiol. 1987; 57:245–259. [PubMed: 3559674]

Dimitrijevic, MR. Motor control in human spinal cord injury. In: Stalberg, E.; Sharma, HS.; Olsson, Y., editors. Spinal Cord Monitoring. Springer; New York: 1998. p. 409-420.

Dougherty BJ, Lee KZ, Lane MA, Reier PJ, Fuller DD. Contribution of the spontaneous crossed-phrenic phenomenon to inspiratory tidal volume in spontaneously breathing rats. J Appl Physiol. 2012; 112:96–105. [PubMed: 22033536]

Duffin J, Iscoe S. The possible role of C5 segment inspiratory interneurons investigated by cross-correlation with phrenic motoneurons in decerebrate cats. Exp Brain Res. 1996; 112:35–40. [PubMed: 8951404]

Edgerton VR, Leon RD, Harkema SJ, Hodgson JA, London N, Reinkensmeyer DJ, Roy RR, Talmadge RJ, Tillakaratne NJ, Timoszyk W, Tobin A. Retraining the injured spinal cord. J Physiol. 2001; 533:15–22. [PubMed: 11351008]

El-Bohy AA, Goshgarian HG. The use of single phrenic axon recordings to assess diaphragm recovery after cervical spinal cord injury. Exp Neurol. 1999; 156:172–179. [PubMed: 10192788]

Ellenberger HH, Feldman JL. Monosynaptic transmission of respiratory drive to phrenic motoneurons from brainstem bulbospinal neurons in rats. J Comp Neurol. 1988; 269:47–57. [PubMed: 3361003]

Ellenberger HH, Feldman JL, Goshgarian HG. Ventral respiratory group projections to phrenic motoneurons: electron microscopic evidence for monosynaptic connections. J Comp Neurol. 1990; 302:707–714. [PubMed: 1707065]

Enriquez Denton M, Wienecke J, Zhang M, Hultborn H, Kirkwood PA. Voltage-dependent amplification of synaptic inputs in respiratory motoneurones. J Physiol. 2012; 590:3067–3090. [PubMed: 22495582]

Flynn JR, Graham BA, Galea MP, Callister RJ. The role of propriospinal interneurons in recovery from spinal cord injury. Neuropharmacology. 2011; 60:809–822. [PubMed: 21251920]

Fuller DD, Baker-Herman TL, Golder FJ, Doperalski NJ, Watters JJ, Mitchell GS. Cervical spinal cord injury upregulates ventral spinal 5-HT2A receptors. J Neurotrauma. 2005; 22:203–213. [PubMed: 15716627]

Fuller DD, Doperalski NJ, Dougherty BJ, Sandhu MS, Bolser DC, Reier PJ. Modest spontaneous recovery of ventilation following chronic high cervical hemisection in rats. Exp Neurol. 2008; 211:97–106. [PubMed: 18308305]

Fuller DD, Johnson SM, Olson EB Jr, Mitchell GS. Synaptic pathways to phrenic motoneurons are enhanced by chronic intermittent hypoxia after cervical spinal cord injury. J Neurosci. 2003; 23:2993–3000. [PubMed: 12684486]

Fuller DD, Sandhu MS, Doperalski NJ, Lane MA, White TE, Bishop MD, Reier PJ. Graded unilateral cervical spinal cord injury and respiratory motor recovery. Respir Physiol Neurobiol. 2009; 165:245–253. [PubMed: 19150658]

Golder FJ, Mitchell GS. Spinal synaptic enhancement with acute intermittent hypoxia improves respiratory function after chronic cervical spinal cord injury. J Neurosci. 2005; 25:2925–2932. [PubMed: 15772352]

Golder FJ, Reier PJ, Bolser DC. Altered respiratory motor drive after spinal cord injury: supraspinal and bilateral effects of a unilateral lesion. J Neurosci. 2001; 21:8680–8689. [PubMed: 11606656]

Goshgarian HG. The role of cervical afferent nerve fiber inhibition of the crossed phrenic phenomenon. Exp Neurol. 1981; 72:211–225. [PubMed: 7202624]

Goshgarian HG. The crossed phrenic phenomenon: a model for plasticity in the respiratory pathways following spinal cord injury. J Appl Physiol. 2003; 94:795–810. [PubMed: 12531916]

Goshgarian HG. The crossed phrenic phenomenon and recovery of function following spinal cord injury. Respir Physiol Neurobiol. 2009; 169:85–93. [PubMed: 19539790]

Goshgarian HG, Yu XJ, Rafols JA. Neuronal and glial changes in the rat phrenic nucleus occurring within hours after spinal cord injury. J Comp Neurol. 1989; 284:519–533. [PubMed: 2768550]

Harkema SJ. Plasticity of interneuronal networks of the functionally isolated human spinal cord. Brain Res Rev. 2008; 57:255–264. [PubMed: 18042493]

Hayashi F, Hinrichsen CF, McCrimmon DR. Short-term plasticity of descending synaptic input to phrenic motoneurons in rats. J Appl Physiol. 2003; 94:1421–1430. [PubMed: 12482770]

Henneman E. Relation between size of neurons and their susceptibility to discharge. Science. 1957; 126:1345–1347. [PubMed: 13495469]

Henneman E, Somjen G, Carpenter DO. Functional Significance of Cell Size in Spinal Motoneurons. J Neurophysiol. 1965; 28:560–580. [PubMed: 14328454]

Kong FJ, Berger AJ. Firing properties and hypercapnic responses of single phrenic motor axons in the rat. J Appl Physiol. 1986; 61:1999–2004. [PubMed: 3027021]

Lane MA. Spinal respiratory motoneurons and interneurons. Respir Physiol Neurobiol. 2011; 179:3–13. [PubMed: 21782981]

Lane MA, Fuller DD, White TE, Reier PJ. Respiratory neuroplasticity and cervical spinal cord injury: translational perspectives. Trends Neurosci. 2008a; 31:538–547. [PubMed: 18775573]

Lane MA, Lee KZ, Fuller DD, Reier PJ. Spinal circuitry and respiratory recovery following spinal cord injury. Respir Physiol Neurobiol. 2009; 169:123–132. [PubMed: 19698805]

Lane MA, Lee KZ, Salazar K, O'Steen BE, Bloom DC, Fuller DD, Reier PJ. Respiratory function following bilateral mid-cervical contusion injury in the adult rat. Exp Neurol. 2012; 235:197–210. [PubMed: 21963673]

Lane MA, White TE, Coutts MA, Jones AL, Sandhu MS, Bloom DC, Bolser DC, Yates BJ, Fuller DD, Reier PJ. Cervical prephrenic interneurons in the normal and lesioned spinal cord of the adult rat. J Comp Neurol. 2008b; 511:692–709. [PubMed: 18924146]

Lee KZ, Fuller DD. Neural control of phrenic motoneuron discharge. Respir Physiol Neurobiol. 2011; 179:71–79. [PubMed: 21376841]

Lee KZ, Reier PJ, Fuller DD. Phrenic motoneuron discharge patterns during hypoxia-induced short-term potentiation in rats. J Neurophysiol. 2009; 102:2184–2193. [PubMed: 19657076]

Lee KZ, Sandhu MS, Dougherty BJ, Reier PJ, Fuller DD. Influence of vagal afferents on supraspinal and spinal respiratory activity following cervical spinal cord injury in rats. J Appl Physiol. 2010; 109:377–387. [PubMed: 20507963]

Li Y, Gorassini MA, Bennett DJ. Role of persistent sodium and calcium currents in motoneuron firing and spasticity in chronic spinal rats. J Neurophysiol. 2004; 91:767–783. [PubMed: 14762149]

Lipski J, Duffin J, Kruszewska B, Zhang X. Upper cervical inspiratory neurons in the rat: an electrophysiological and morphological study. Exp Brain Res. 1993; 95:477–487. [PubMed: 8224074]

Mantilla CB, Bailey JP, Zhan WZ, Sieck GC. Phrenic motoneuron expression of serotonergic and glutamatergic receptors following upper cervical spinal cord injury. Exp Neurol. 2012; 234:191–199. [PubMed: 22227062]

Mantilla CB, Sieck GC. Invited review: Mechanisms underlying motor unit plasticity in the respiratory system. J Appl Physiol. 2003; 94:1230–1241. [PubMed: 12571144]

Mantilla CB, Sieck GC. Neuromuscular adaptations to respiratory muscle inactivity. Respir Physiol Neurobiol. 2009; 169:133–140. [PubMed: 19744580]

Mantilla CB, Sieck GC. Phrenic motor unit recruitment during ventilatory and non-ventilatory behaviors. Respir Physiol Neurobiol. 2011; 179:57–63. [PubMed: 21763470]

Monteau R, Khatib M, Hilaire G. Central determination of recruitment order: intracellular study of phrenic motoneurons. Neurosci Lett. 1985; 56:341–346. [PubMed: 4022446]

Murray KC, Nakae A, Stephens MJ, Rank M, D'Amico J, Harvey PJ, Li X, Harris RL, Ballou EW, Anelli R, Heckman CJ, Mashimo T, Vavrek R, Sanelli L, Gorassini MA, Bennett DJ, Fouad K.

Recovery of motoneuron and locomotor function after spinal cord injury depends on constitutive activity in 5-HT2C receptors. Nat Med. 2010; 16:694–700. [PubMed: 20512126]

Murray KC, Stephens MJ, Ballou EW, Heckman CJ, Bennett DJ. Motoneuron excitability and muscle spasms are regulated by 5-HT2B and 5-HT2C receptor activity. J Neurophysiol. 105:731–748. [PubMed: 20980537]

Olson EB Jr, Bohne CJ, Dwinell MR, Podolsky A, Vidruk EH, Fuller DD, Powell FL, Mitchel GS. Ventilatory long-term facilitation in unanesthetized rats. J Appl Physiol. 2001; 91:709–716. [PubMed: 11457785]

Rowley KL, Mantilla CB, Sieck GC. Respiratory muscle plasticity. Respir Physiol Neurobiol. 2005; 147:235–251. [PubMed: 15871925]

Sandhu MS, Dougherty BJ, Lane MA, Bolser DC, Kirkwood PA, Reier PJ, Fuller DD. Respiratory recovery following high cervical hemisection. Respir Physiol Neurobiol. 2009; 169:94–101. [PubMed: 19560562]

Sieck GC, Mantilla CB. Role of neurotrophins in recovery of phrenic motor function following spinal cord injury. Respir Physiol Neurobiol. 2009; 169:218–225. [PubMed: 19703592]

Sperry MA, Goshgarian HG. Ultrastructural changes in the rat phrenic nucleus developing within 2 h after cervical spinal cord hemisection. Exp Neurol. 1993; 120:233–244. [PubMed: 7684001]

St John WM, Bartlett D Jr. Comparison of phrenic motoneuron responses to hypercapnia and isocapnic hypoxia. J Appl Physiol. 1979; 46:1096–1102. [PubMed: 468630]

St John WM, Bartlett D Jr. Comparison of phrenic motoneuron activity during eupnea and gasping. J Appl Physiol. 1981; 50:994–998. [PubMed: 6785268]

St John WM, Bartlett D Jr. Comparison of phrenic motoneuron activity in eupnea and apneusis. Respir Physiol. 1985; 60:347–355. [PubMed: 4035110]

Stornetta RL, Sevigny CP, Guyenet PG. Inspiratory augmenting bulbospinal neurons express both glutamatergic and enkephalinergic phenotypes. J Comp Neurol. 2003; 455:113–124. [PubMed: 12455000]

Sukiasyan N, Hultborn H, Zhang M. Distribution of calcium channel Ca(V)1.3 immunoreactivity in the rat spinal cord and brain stem. Neuroscience. 2009; 159:217–235. [PubMed: 19136044]

Tai Q, Palazzolo K, Mautes A, Nacimiento W, Kuhtz-Buschbeck JP, Nacimiento AC, Goshgarian HG. Ultrastructural characteristics of glutamatergic and GABAergic terminals in cat lamina IX before and after spinal cord injury. J Spinal Cord Med. 1997a; 20:311–318. [PubMed: 9261776]

Tai Q, Palazzolo KL, Goshgarian HG. Synaptic plasticity of 5-hydroxytryptamine-immunoreactive terminals in the phrenic nucleus following spinal cord injury: a quantitative electron microscopic analysis. J Comp Neurol. 1997b; 386:613–624. [PubMed: 9378855]

Tian GF, Peever JH, Duffin J. Synaptic connections to phrenic motoneurons in the decerebrate rat. Adv Exp Med Biol. 1998; 450:51–59. [PubMed: 10026963]

Vinit S, Stamegna JC, Boulenguez P, Gauthier P, Kastner A. Restorative respiratory pathways after partial cervical spinal cord injury: role of ipsilateral phrenic afferents. Eur J Neurosci. 2007; 25:3551–3560. [PubMed: 17610574]

Webber CL Jr, Pleschka K. Structural and functional characteristics of individual phrenic motoneurons. Pflugers Arch. 1976; 364:113–121. [PubMed: 60738]

Zhang M, Moller M, Broman J, Sukiasyan N, Wienecke J, Hultborn H. Expression of calcium channel CaV1.3 in cat spinal cord: light and electron microscopic immunohistochemical study. J Comp Neurol. 2008; 507:1109–1127. [PubMed: 18095323]

Zimmer MB, Goshgarian HG. Spinal cord injury in neonates alters respiratory motor output via supraspinal mechanisms. Exp Neurol. 2007; 206:137–145. [PubMed: 17559837]

Zimmer MB, Nantwi K, Goshgarian HG. Effect of spinal cord injury on the respiratory system: basic research and current clinical treatment options. J Spinal Cord Med. 2007; 30:319–330. [PubMed: 17853653]

Highlights

- First description of phrenic motoneuron burst patterns after chronic spinal injury
- Most cells were either silent or active late in the inspiratory period
- Discharge patterns returned towards control values by 8 wks post-injury
- A novel pattern was noted in which some cells burst tonically during apnea

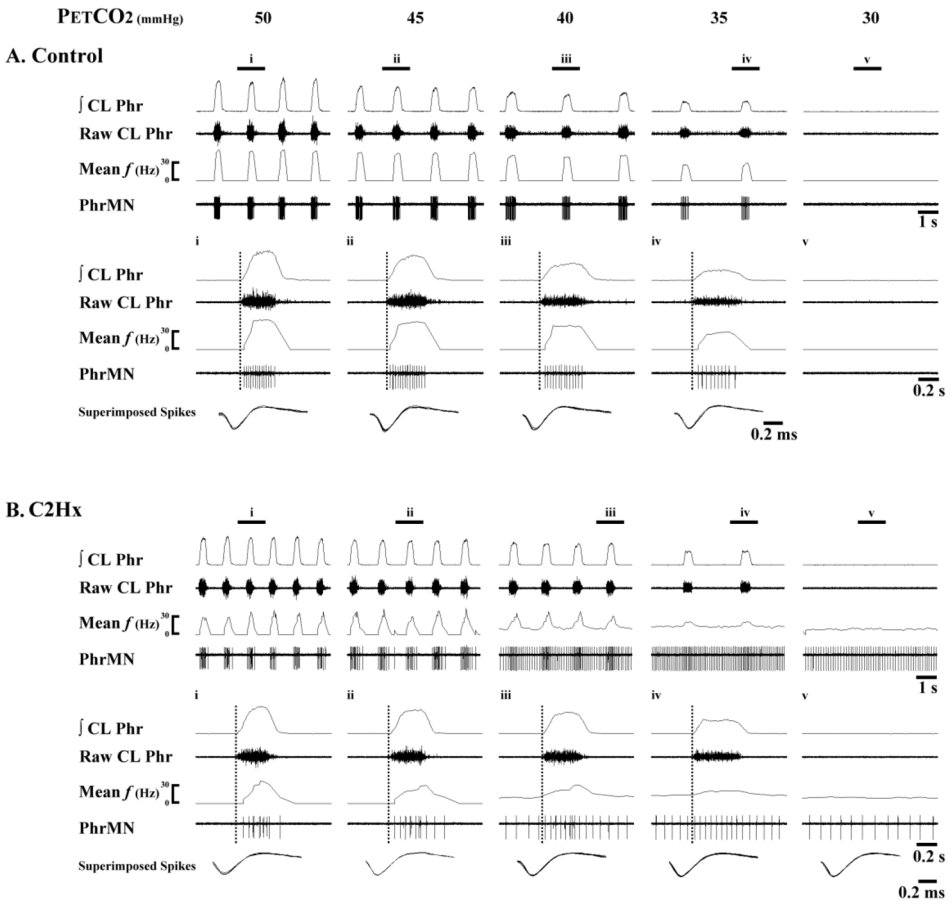

Fig. 1. Representative examples of Early-I PhMN bursting

Data are shown from a spinal-intact control rat (**A**) and another at 8 wk post-C2Hx (**B**). Within each panel, the top traces show several respiratory cycles, and the bottom traces show an expanded trace depicting a single neural breath from the area marked *i* through *v*. Both PhMN burst frequency (mean *f*) and raw spikes are presented along with the raw and integrated (∫) contralateral phrenic nerve recording (CL Phr). The vertical dotted lines represent the onset of the inspiratory burst recorded in the contralateral phrenic nerve. In this example, PhMNs began bursting within the first 20% of the inspiratory period and accordingly were defined as Early-I PhMNs. In the control animal, Early-I PhMN discharge declines as $P_{ET}CO_2$ is reduced and eventually ceases firing when apnea is observed in the CL phrenic nerve recording. In contrast, in the C2Hx animal note that inspiratory bursting gradually transforms into a tonic discharge pattern as $P_{ET}CO_2$ is reduced, and bursting continues during the period of inspiratory apnea. The traces labeled “Superimposed spikes” show a superimposition of the individual PhMN spikes and are provided to illustrate that the recordings are from the same neuron.

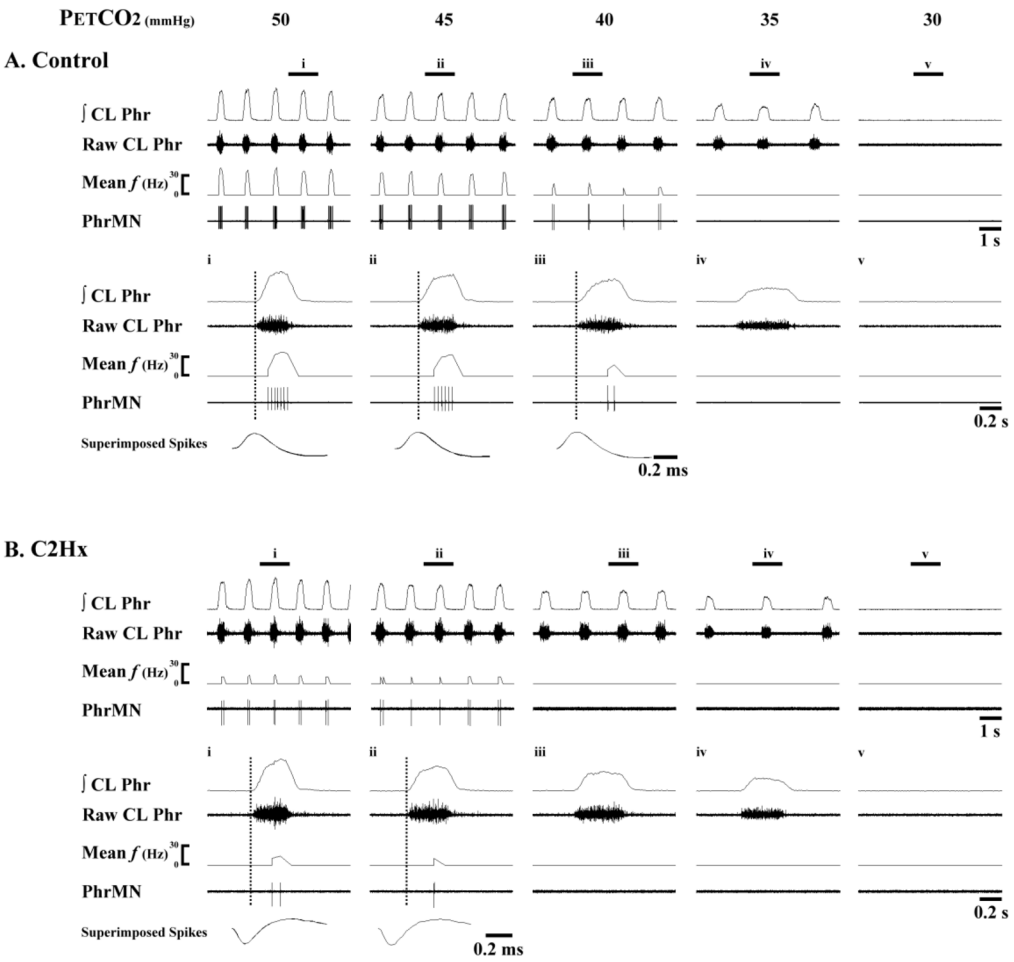

Fig. 2. Representative examples of Late-I PhMN bursting

Data are shown from a spinal-intact control rat (**A**) and another at 8 wk post-C2Hx (**B**). Within each panel, the top traces show several respiratory cycles, and the bottom traces show an expanded trace depicting a single neural breath from the area marked *i* through *v*. Both PhMN burst frequency (mean *f*) and raw spikes are presented along with the raw and integrated (∫) contralateral phrenic nerve recording (CL Phr). The vertical dotted lines represent the onset of the inspiratory burst recorded in the contralateral phrenic nerve. In this example, PhMNs began firing after the initial 20% of the inspiratory period and were therefore defined as Late-I PhMNs. In both the control and C2Hx animal, Late-I PhMN discharge declines as $P_{ET}CO_2$ is reduced and eventually ceases firing before apnea is observed in the CL phrenic nerve recording. Note the reduced mean *f* in the C2Hx animal as compared to the control animal. The superimposed spikes provide an overlay of individual PhMN spikes to illustrate that the recordings are from the same neuron.

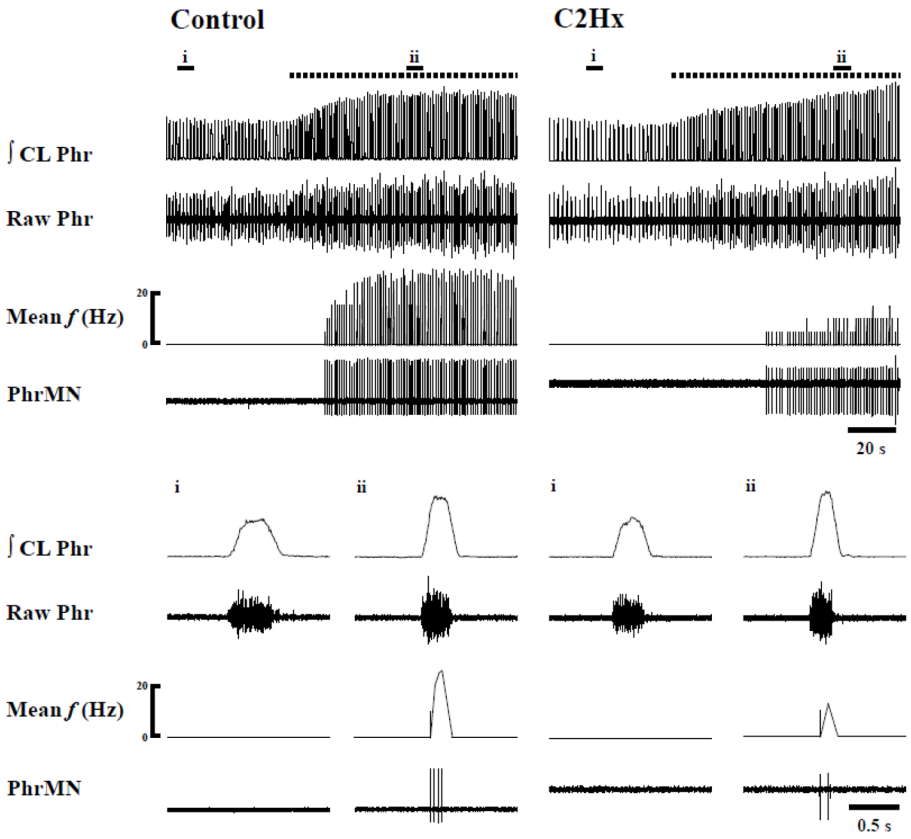

Fig. 3. Representative recordings which demonstrate recruitment of initially silent PhMNs during a hypercapnic challenge

Data are shown from a spinal-intact control rat (left) and another at 2 wk post-C2Hx (right). The lower panels marked *i* and *ii* provide expanded time scale traces depicting a single neural breath. The horizontal dotted line represents the period of hypercapnic stimulation. ∫CL: integrated contralateral phrenic nerve activity.

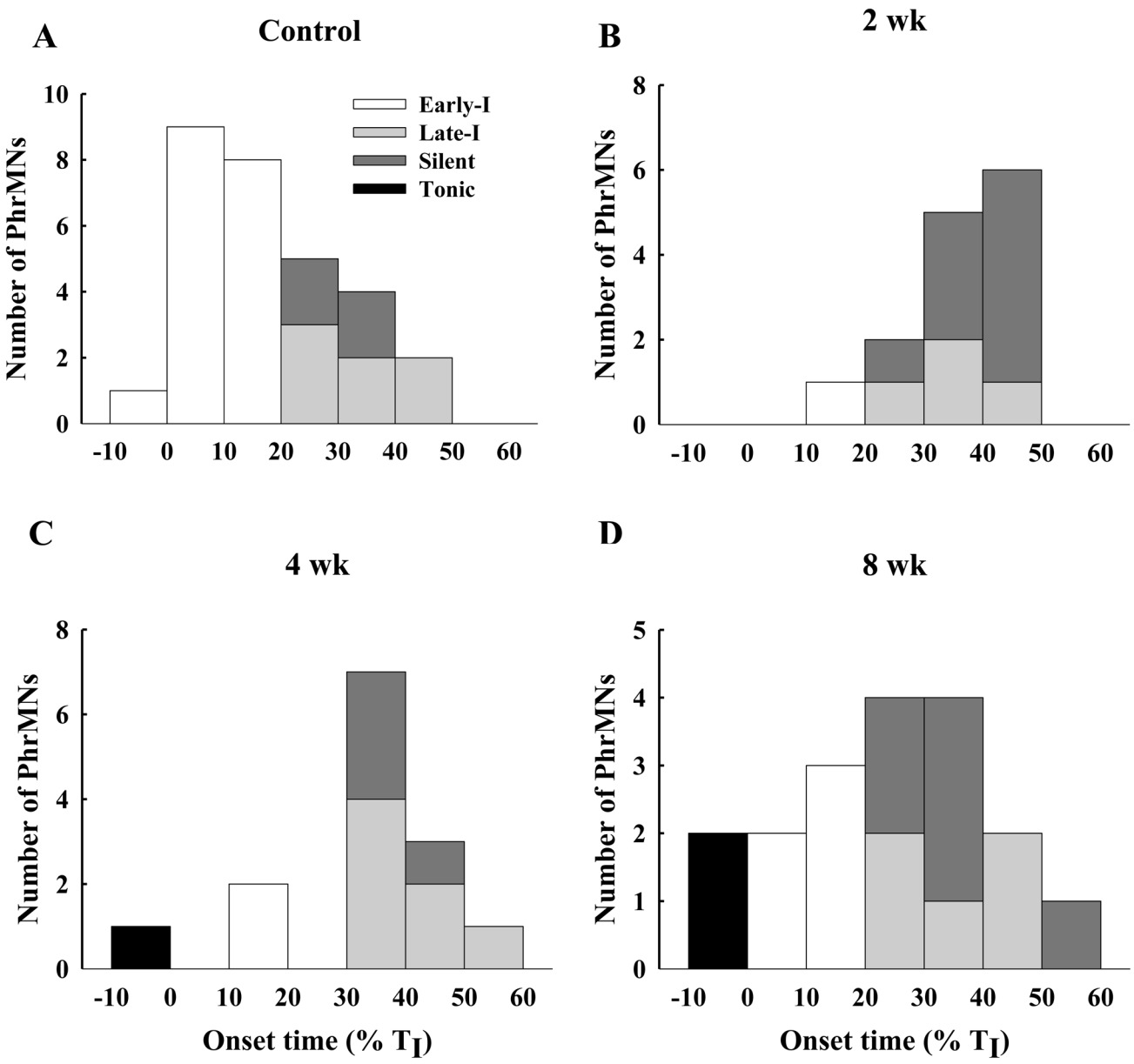

Fig. 4. The distribution of PhMN discharge onset values in control (A), 2 wk (B), 4 wk (C) and 8 wk (D) post-C2Hx animals

The onset of PhMN bursting is represented as percentage of the total inspiratory duration (i.e., % T_I). Active PhMNs were classified as Early-I (white bars), Late-I (light grey bars) and tonic (black bars) while $P_{ET}CO_2$ was maintained at a value of 50 mmHg. Those PhMNs classified as silent (dark grey bars) were not active under baseline conditions, but were recruited during a respiratory challenge ($P_{ET}CO_2$ ~ 70–80 mmHg).

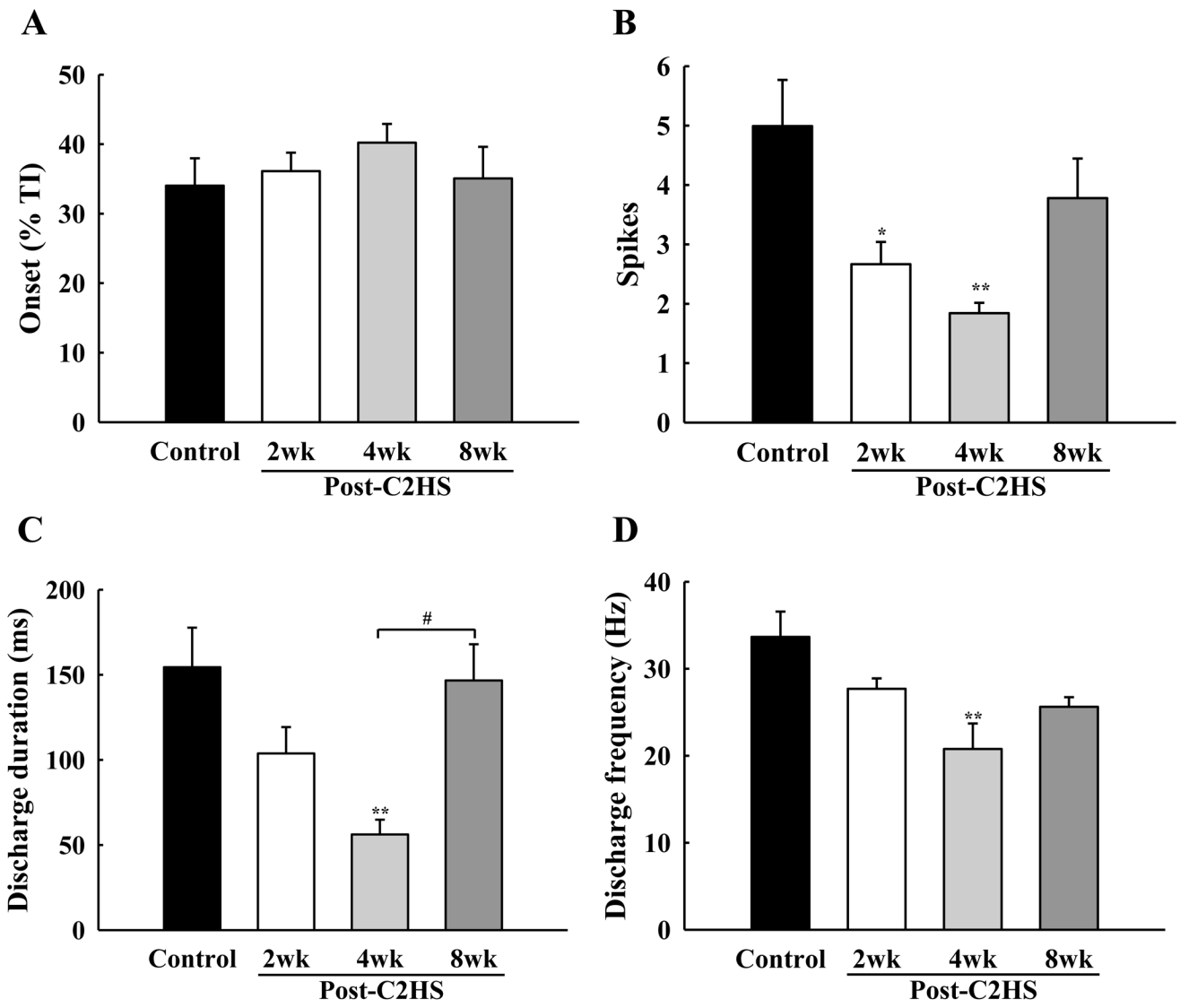

Fig. 5. Mean discharge patterns of Late-I PhMNs

The discharge onset time (**A**), spikes per neural breath (**B**), discharge duration (**C**) and discharge frequency (**D**) were quantified in control, 2 wk, 4 wk and 8 wk post-C2Hx animals at 50 mmHg $P_{ET}CO_2$. * $P < 0.05$; **: $P < 0.01$ significant difference vs. control; #: $P < 0.05$ significant difference between 4 wk and 8 wk groups.

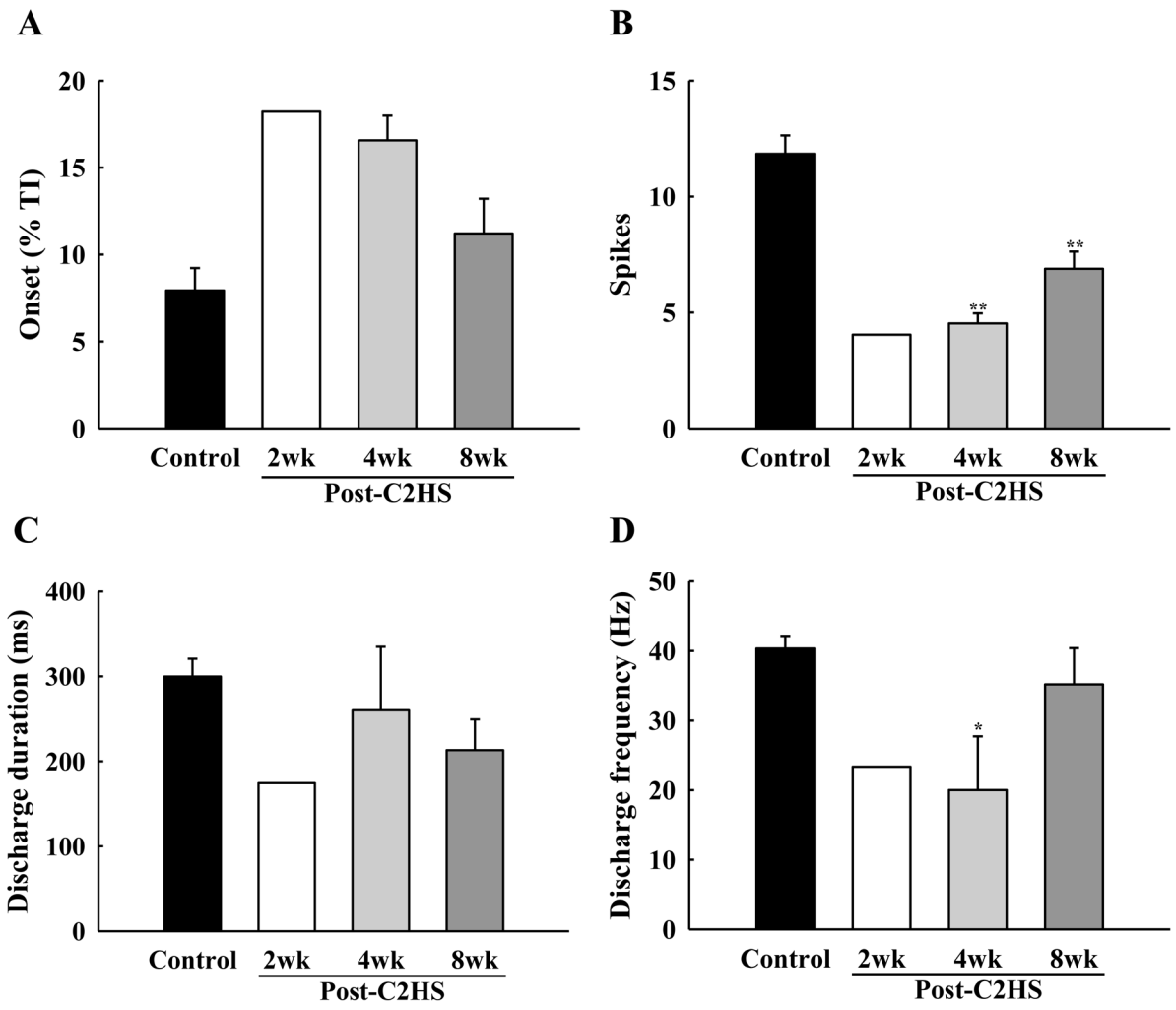

Fig. 6. Mean discharge patterns of Early-I PhMNs

The discharge onset time (**A**), spikes per neural breath (**B**), discharge duration (**C**) and discharge frequency (**D**) were quantified in control, 2 wk, 4 wk and 8 wk post-C2Hx animals at 50 mmHg $P_{ET}CO_2$. * $P < 0.05$; **: $P < 0.01$ significant difference vs. control.

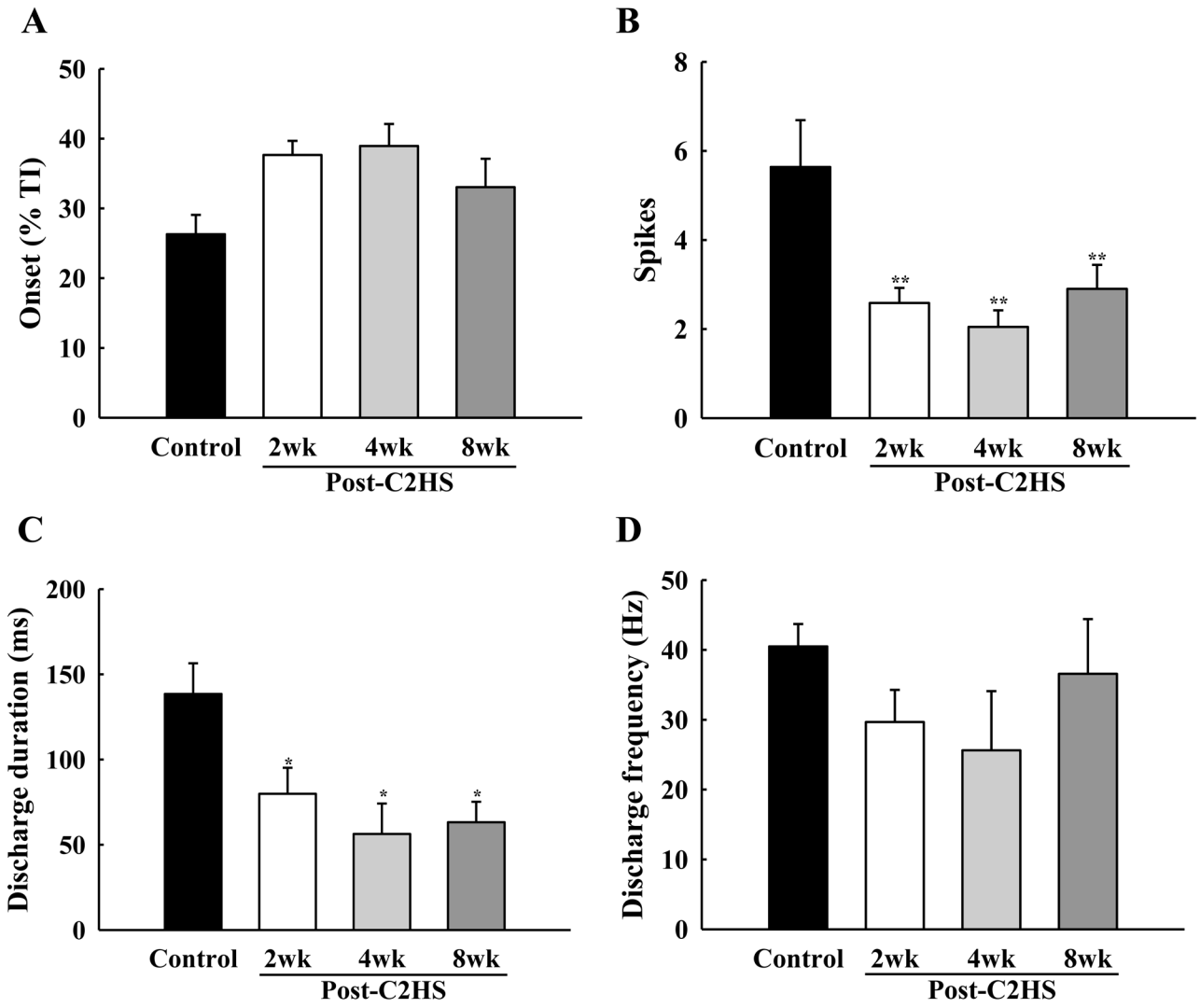

Fig. 7. Mean discharge patterns of initially silent PhMNs

These silent PhMNs were recruited during respiratory stimulation with hypercapnia ($P_{ET}CO_2$ ~ 70–80 mmHg). The discharge onset time (**A**), spikes per neural breath (**B**), discharge duration (**C**) and discharge frequency (**D**) were quantified in control, 2 wk, 4 wk and 8 wk post-C2Hx animals. * $P < 0.05$; **: $P < 0.01$ significant difference vs. control

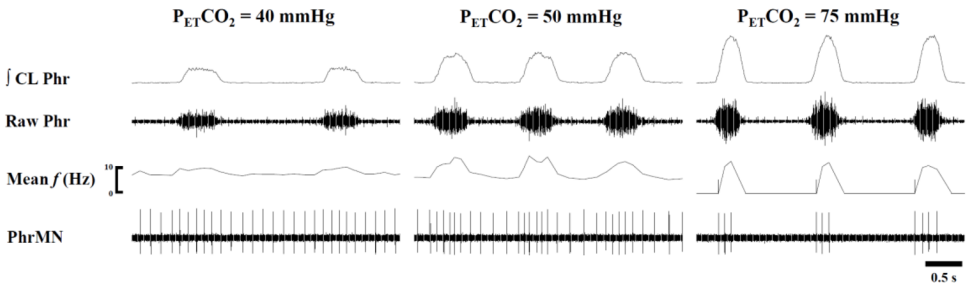

Fig. 8. Representative example illustrating that tonic PhMN bursting patterns are dependent upon the level of respiratory drive

This example shows three different levels of $P_{ET}CO_2$ and was obtained 4 week post-C2Hx. PhMN burst frequency (mean *f*) and raw spikes are presented along with the contralateral (CL) phrenic nerve burst. In this example, the PhMN can be seen to burst across the respiratory cycle but with a clear phasic inspiratory modulation during normocapnia ($P_{ET}CO_2$ = 50 mmHg). This inspiratory modulatory effect was attenuated at a lower $P_{ET}CO_2$ level, and increasing $P_{ET}CO_2$ to 75 mmHg eliminated the tonic activity.

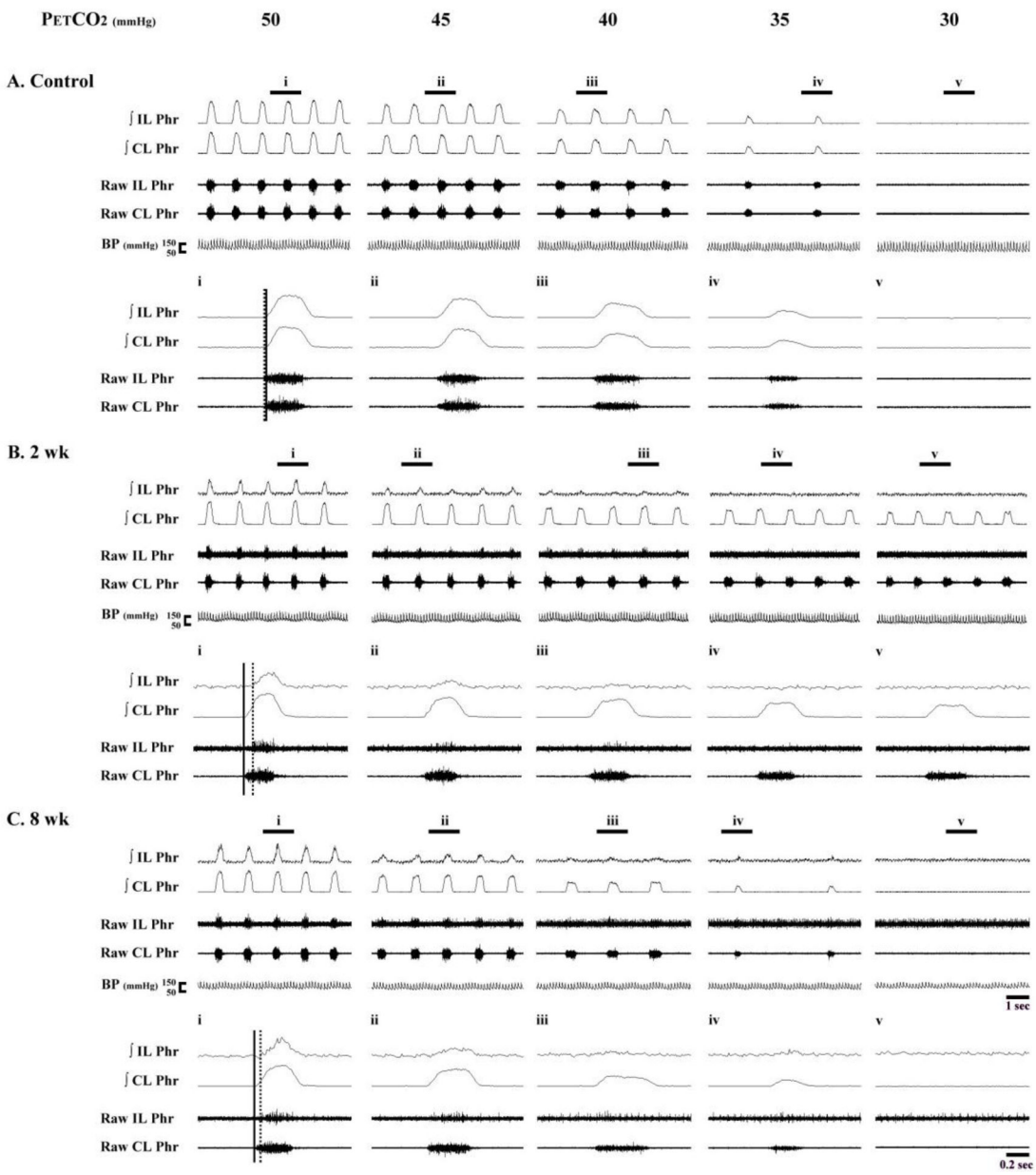

Fig. 9. Representative examples of bilateral phrenic nerve activity

Data are presented from a control rat (**A**), and additional rats studied at 2 weeks (2 wk, **B**) and 8 weeks (8 wk, **C**) post-C2Hx. Expanded time scale traces depicting a single neural breath are indicated by the panels labeled *i* – *v*. Both integrated (∫) and raw phrenic nerve activity is shown. The vertical solid and dotted line are provided to indicate the discharge onset of the contralateral and ipsilateral phrenic burst, respectively.

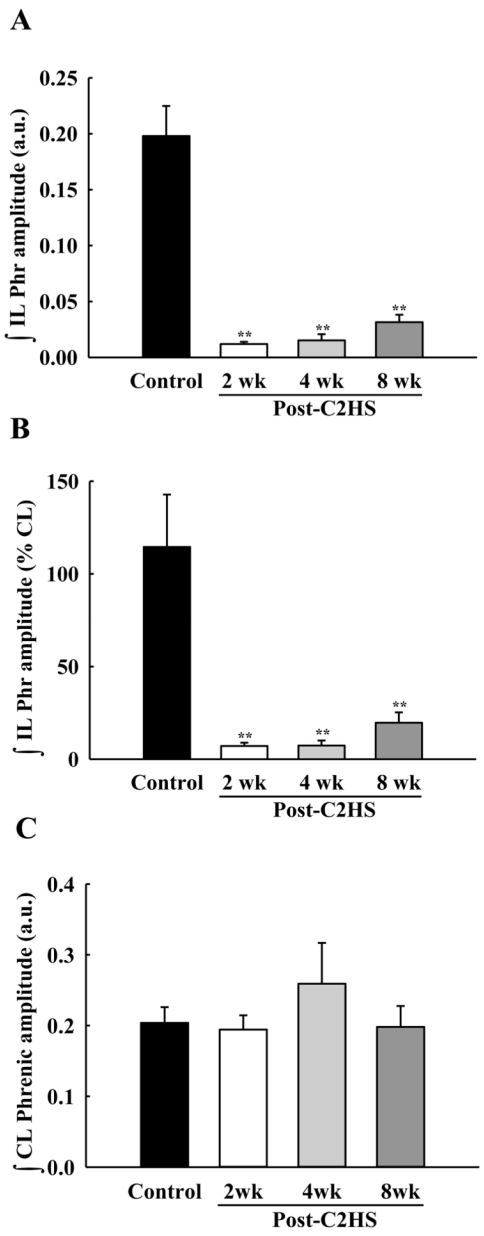

Fig. 10. Mean phrenic nerve burst amplitude during baseline conditions

Data were collected with $P_{ET}CO_2$ held at 50 mmHg, and are shown for the ipsilateral (∫IL)and contralateral (∫CL) nerve recordings in control and C2Hx animals. Burst amplitude is presented as arbitrary units (a.u., panel A and C) and also normalized to the contralateral phrenic burst amplitude (% CL, panel B). Ipsilateral phrenic burst amplitude was significantly reduced in all C2Hx groups while contralateral phrenic bursting was similar across groups. **: $P < 0.01$ different than control animals.

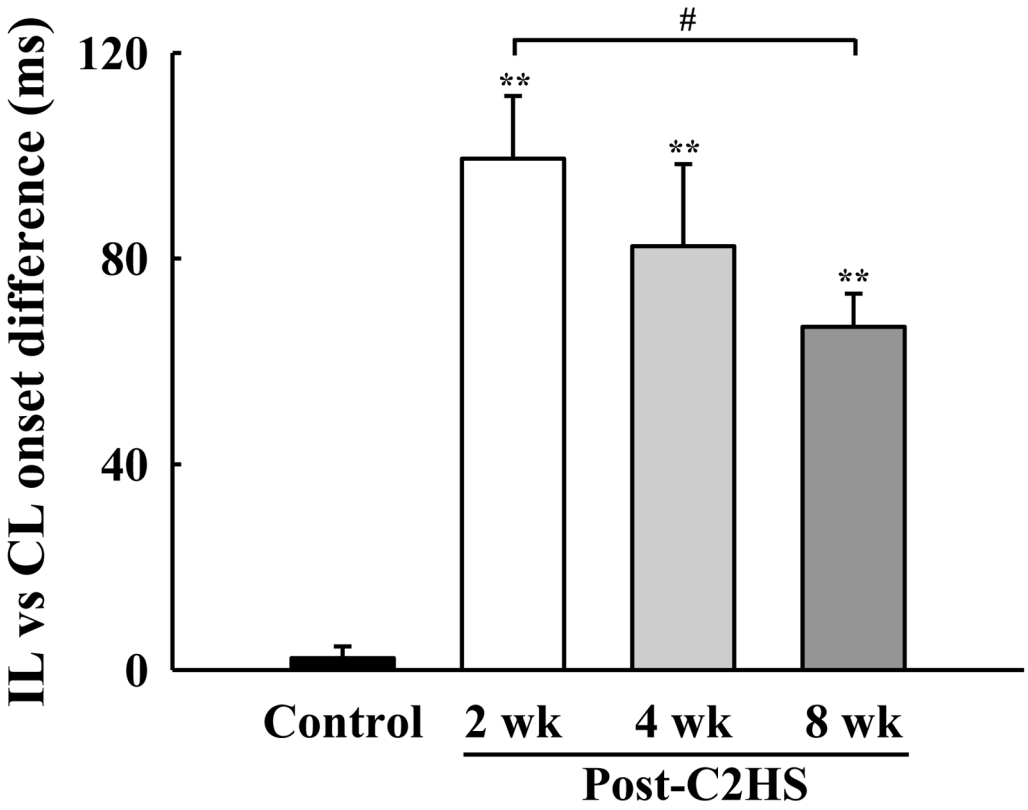

Fig. 11. Mean difference in the discharge onset between the ipsilateral (IL) and contralateral (CL) phrenic nerve inspiratory bursts

The onset of the ipsilateral phrenic burst occurred after the contralateral burst in all C2Hx animals. However, the onset difference gradually decreased over time post-injury. **: $P < 0.01$ different than control; #: $P < 0.05$ difference between 2 and 8 wk post-C2Hx groups.

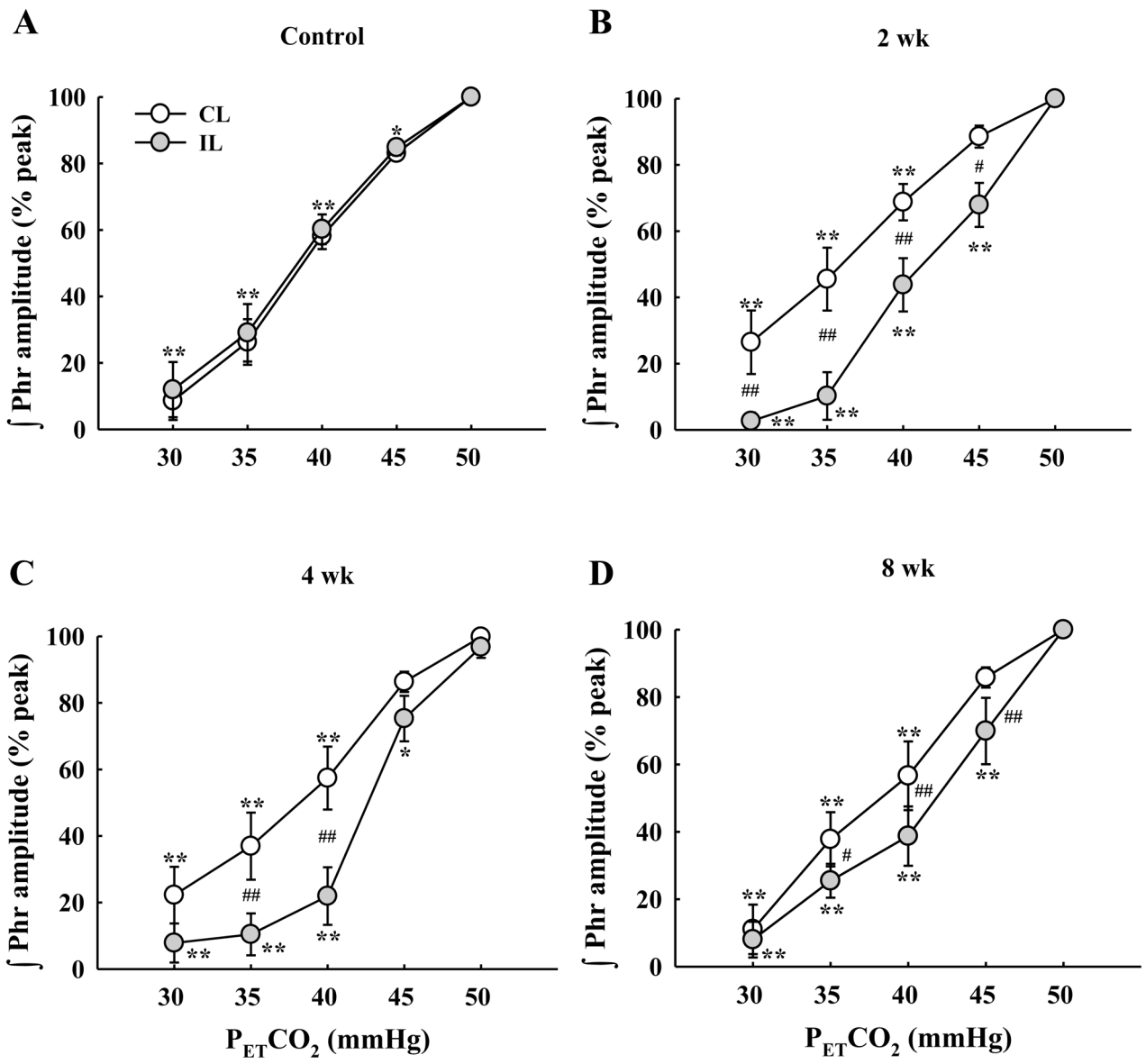

Fig. 12. Mean changes in the phrenic neurogram inspiratory burst amplitude as $P_{ET}CO_2$ was gradually changed

Each panel shows data from the ipsilateral (IL) and contralateral (CL) phrenic nerves in control (**A**), 2 wk (**B**), 4 wk (**C**) and 8 wk (**D**) post-C2Hx animals. All groups showed a progressive reduction in the burst amplitude of both phrenic nerves in parallel with $P_{ET}CO_2$ reductions. Changes in bursting were indistinguishable between the two phrenic nerves in control rats (**A**). In contrast, the ipsilateral phrenic burst declined more severely in as $P_{ET}CO_2$ was reduced in C2Hx animals. *: $P < 0.05$; **: $P < 0.01$ different from 50 mmHg data point. #: $P < 0.05$; ##: $P < 0.01$ difference between the ipsilateral and contralateral burst amplitude at the same level $P_{ET}CO_2$.

Table 1

Mean arterial blood pressure (MAP) and heart rate (HR) in control, 2 wk, 4 wk and 8 wk post-C2HS animals under different levels of $P_{ET}CO_2$

MAP (mmHg)

	$P_{ET}CO_2$ (mmHg)				
	30	**35**	**40**	**45**	**50**
Control	97 ± 7**	105 ± 5	107 ± 5	109 ± 5	110 ± 5
2 wk	98 ± 2**	103 ± 3**	111 ± 3	114 ± 3	114 ± 4
4 wk	92 ± 3**	100 ± 3**	104 ± 3	107 ± 3	108 ± 3
8 wk	93 ± 6**	96 ± 6	97 ± 5	98 ± 6	100 ± 6

HR (beats/min)

	$P_{ET}CO_2$ (mmHg)				
	30	35	40	45	50
Control	462 ± 14**	442 ± 7	442 ± 7	439 ± 8	436 ± 8
2 wk	449 ± 9	450 ± 9	451 ± 9	450 ± 8	449 ± 8
4 wk	439 ± 12*	432 ± 9	432 ± 12	425 ± 13	421 ± 11
8 wk	433 ± 8	437 ± 9	432 ± 9	428 ± 9	424 ± 9

Values are mean ± SE.

* $P < 0.05$;

** $P < 0.01$ compared with the value at 50 mmHg $P_{ET}CO_2$

Exp Neurol. Author manuscript; available in PMC 2014 November 01.

Table 2

Discharge frequency of Late-I PhMNs in control, 2 wk, 4 wk and 8 wk post-C2HS animals under different levels of $P_{ET}CO_2$

	$P_{ET}CO_2$ (mmHg)				
	30	**35**	**40**	**45**	**50**
Control	0 ± 0 **	2.8 ± 2.8 **	7.2 ± 3.5 **	20.6± 5.7 **	33.7± 2.9
2 wk	0 ± 0 **	6.8 ± 6.8 **	6.6 ± 6.6 **	29.8 ± 5.4	27.7 ± 1.2
4 wk	0 ± 0 **	0 ± 0 **	8.1 ± 3.5 **	11.2 ± 3.6 *	20.8 ± 2.9 #
8 wk	4.3 ± 4.3 **	4.5 ± 4.5 **	6.7 ± 4.2 **	12.2 ± 5.8 **	25.6 ± 1.1

Values are mean ± SE.

* P < 0.05;

** P < 0.01 compared with the value at 50 mmHg $P_{ET}CO_2$.

# P < 0.05 compared with the value from control animals.

Exp Neurol. Author manuscript; available in PMC 2014 November 01.

Table 3

Respiratory frequency in control, 2 wk, 4 wk and 8 wk post-C2Hx animals under different levels of $P_{ET}CO_2$

	$P_{ET}CO_2$ (mmHg)				
	30	**35**	**40**	**45**	**50**
Control	4 ± 2 **	9 ± 3 **	26 ± 3 **	37 ± 2 **	46 ± 2
2 wk	21 ± 7 **, #	29 ± 6 **, ##	34 ± 4 **	43 ± 3	49 ± 2
4 wk	17 ± 7 **, #	24 ± 6 **, #	32 ± 6 **	45 ± 3	49 ± 2
8 wk	8 ± 6 **	19 ± 6 **	31 ± 6 **	50 ± 3	54 ± 3

Values are mean ± SE.

* $P < 0.05$;

** $P < 0.01$ compared with the value at 50 mmHg $P_{ET}CO_2$.

# $P < 0.05$;

$P < 0.01$ compared with the value from control animals.